Finite element software for practical EMI problems

Shinji Tanabe[1], Yuichiro Murata[1], Yoichi Nojima[2], Yoshifumi Tanaka[2] and Adalbert Konrad[3]
[1]*Advanced Technology R&D Center, Mitsubishi Electric Corporation*
8-1-1 Tsukaguchi-Honmachi, Amagasaki, Hyogo 661, Japan
tanabe@ele.crl.melco.co.jp
[2]*CRC Research Institute, Inc., Tokyo, Japan*
[3]*University of Toronto, Dept. of E.C.E., Toronto, Canada*

Abstract

MAGNA/EMI is a finite element code based on the coupled $\vec{A} - \phi$ method for three-dimensional electromagnetic (EM) field analysis. The paper describes this four-component vector/scalar potential formulation in some detail. It explains how to choose the gauge condition for each application model and how to set the electric and magnetic field directions on the boundary surfaces. The perfectly matched layer (PML) concept is used as the absorbing boundary condition (ABC). The accuracy of results is confirmed by comparison with analytical solutions for the voltage standing wave ratio (VSWR) and skin depth computation. Computed and analytical values agree well even when the finite element aspect ratio is less than optimal. Both incomplete Cholesky conjugate gradient (ICCG) and Gauss-type equation solvers are available with MAGNA/EMI. A comparison of the solvers is made for both geometrical and electrical bad aspect ratio problems. Two practical applications, cellular phone shield-design and electromagnetic resonance inside a car, are presented as examples. They demonstrate that MAGNA/EMI is a valuable tool in the hands of EMI/EMC engineers.

1 Introduction

There are three main methods which can be used as computation tools for electromagnetic interference (EMI): (i) the Method of Moments (MoM), (ii) the

Finite Difference Time Domain (FDTD) method, and (iii) the Finite Element Method (FEM). Each method has its advantages and disadvantages. For example, MoM cannot treat the inside of materials and FDTD cannot treat bad aspect ratio rectangular elements. Thus it is impossible to model thin layers of conductors, which are used on printed circuit boards (PCB's) and for shielding, because the computation time is prohibitively long unless the perfect electric conductor (PEC) assumption is used.

The FEM is a very effective method for single frequency, steady state problems. For high frequency analysis, a wave equation rather than diffusion equation needs to be solved. Therefore, not only induced fields but also radiation EM fields must be considered. Since the latter will transfer Poynting energy to infinite space, absorbing boundaries are necessary to truncate the computation region. An integral equation is required to obtain the fields outside the computation region.

EMI is usually measured in the 30MHz to 1GHz frequency-range. The noise source to antenna distance is usually 3m or 10m where the antenna detects both near and far fields of comparable magnitudes. Since the electric field phases of EMI noise signals are at random, it is almost impossible to analyze EMI noise at the antenna position without recourse to numerical methods.

We developed a FEM code to analyze EMI problems and confirmed its accuracy by comparing with analytical solutions in some basic cases. The code has been applied to the design of shields and PCB's.

2 Numerical model

2.1 Basic equations

A three-dimensional FEM (Tanabe [1]) is used in the analysis. From Faraday's law and Gauss' law for magnetic fields, the electric scalar potential ϕ and the magnetic vector potential $\vec{A}$ are defined as follows:

$$\vec{E} = -\frac{\partial \vec{A}}{\partial t} - grad\phi \tag{1}$$

$$\vec{B} = curl\vec{A} \tag{2}$$

From Ampere's law and the continuity equation, the following equations for $\vec{A}$ and ϕ are obtained,

$$curl\frac{1}{\mu}curl\vec{A} - (\sigma + \frac{\partial}{\partial t}\varepsilon)(\frac{\partial \vec{A}}{\partial t} + grad\phi) = 0 \tag{3}$$

$$div(\sigma + \varepsilon\frac{\partial}{\partial t})(\frac{\partial \vec{A}}{\partial t} + grad\phi) = -\frac{\partial \rho_v}{\partial t} \tag{4}$$

where μ, ε, σ and ρ_v are permeability, permittivity, conductivity and volume

electric charge density, respectively. The above generalized vector and scalar wave equations constitute the system of differential equations which form the basis of the MAGNA/EMI finite element program. For time-harmonic vector and scalar potentials and in the absence of space charges, (3) and (4) become:

$$curl\frac{1}{\mu}curl\vec{A}-(\sigma+j\omega\varepsilon)(j\omega\vec{A}+grad\phi)=0 \tag{5}$$

$$div(\sigma+j\omega\varepsilon)(j\omega\vec{A}+grad\phi)=0 \tag{6}$$

MAGNA/EMI employs linear interpolation functions to approximate the unknown solution within first-order hexagonal finite elements having eight nodes. To formulate the system equations, Galerkin's method is used and the following deterministic type matrix equation is obtained

$$[S]\left[\begin{matrix}\vec{A}\\ \phi\end{matrix}\right]=[b] \tag{7}$$

[*S*] is a 4N×4N symmetric global finite element coefficient matrix with N being the total number of finite element nodes. Each element of the matrix consists of known complex values. Since each node in the finite element mesh may be surrounded by eight finite elements, there can be as many as 4×27 = 108 non-zero terms in each row or column of [*S*]. The right-hand side of (7), [*b*], is a given 4N×1 column matrix for excitations. The unknowns, $\vec{A}$ and ϕ, are obtained from the system equations in the form of complex phasors. Therefore, eddy currents in regions with finite conductivity and displacement currents in dielectric media are considered automatically. In order to solve (7), both the ICCG and Gauss methods are available with MAGNA/EMI. The ICCG solver requires much less CPU time and computer memory than the Gauss solver. However, there is the possibility of a non-converging solution in those situations where bad aspect ratio finite elements are unavoidable. A detailed comparison of the two solvers, particularly for bad aspect ratio problems, is given in Section 7.

3 Gauges

MAGNA/EMI uses $\vec{A}$ and ϕ as the unknowns. Therefore, to fix the values uniquely, a gauge condition should be imposed. In MAGNA/EMI, the gauge condition is introduced in conjunction with the boundary conditions for ϕ. For example, when inputting a noise source, a scalar potential, which varies like a wave on the problem boundary, is equivalent to the Lorentz gauge given by

$$div\vec{A}+\mu\varepsilon\frac{\partial\phi}{\partial t}=0 \tag{8}$$

On the other hand, constraining ϕ to be constant on the boundary leads to the Coulomb gauge, i.e.

$$div\vec{A} = 0 . \tag{9}$$

A practical example of imposing the gauge condition for inputting a plain wave is given in Section 5.

4 Boundary conditions

4.1 Dirichlet and Neumann boundary conditions

The directions of the electric and magnetic fields on the boundary will be decided by the boundary conditions for $\vec{A}$ and ϕ. The natural (Neumann) boundary conditions available in MAGNA/EMI are

$$\vec{n} \times \frac{1}{\mu} curl\vec{A} = 0 \qquad \text{(normal } \vec{H}\text{)} \tag{10a}$$

$$\vec{n} \cdot (j\omega\vec{A} + grad\phi) = 0 \qquad \text{(tangential } \vec{E}\text{)} \tag{10b}$$

For example, if the *xy*-plane is a *perfect electric conductor* boundary, then the Dirichlet boundary conditions $A_x = A_y = 0$ and $\phi = constant$ on the *xy*-plane mean that the electric field $\vec{E}$ is normal to the plane, while by (2) the magnetic field $\vec{H}$ is parallel to the plane. Now consider a *perfect magnetic conductor* boundary at the *xy*-plane. From (10b), the Dirichlet boundary condition $A_z = 0$ and the Neumann boundary condition $d\phi / dn = 0$ on the *xy*-plane mean that the electric field $\vec{E}$ is tangential to the plane. At the same time, by virtue of (10a), the Dirichlet boundary condition $A_z = 0$ and the Neumann boundary conditions $dA_x / dn = dA_x / dz = 0$ and $dA_y / dn = dA_y / dz = 0$ will make the magnetic field $\vec{H}$ perpendicular to the *xy*-plane.

4.2 Absorbing boundary condition

An absorbing layer should be added around the analysis region in a FEM EM field analysis. In order to absorb the radiated EM energy at the boundary, a boundary condition similar to Berenger's PML (Berenger [2]) of the FDTD method has been used. The energy should be absorbed in the boundary layer with electric conductivity σ and magnetic loss σ^*; the latter is defined in terms of the imaginary part of the complex permeability μ'', by the following equation

$$\sigma^* = j\omega\mu'' \tag{11}$$

The magnetic loss σ^* will be input in the form of the imaginary part of the permeability μ'' because it is convenient to input the properties of magnetic materials from measured results. In order to reduce the reflection of the wave energy, the characteristic impedance of free space and that of the layer should be matched; therefore, the following condition must be satisfied:

$$\frac{\sigma}{\varepsilon_o} = \frac{\sigma^*}{\mu_o} \tag{12}$$

where ε_o and μ_o are free space permittivity and permeability, respectively. The sudden change in σ and σ^* causes numerical computation errors. The choice of the value of σ is very critical for minimizing the reflection. For sufficient absorption, at least three or four absorbing layers are needed.

4.3 Combination with Green's function

The FEM has many advantages in EM field calculation but one of its disadvantages is that it requires the meshing of the whole calculation region. Therefore, it is practically impossible to obtain the field values at the antenna position in an anechoic chamber or an open site. However, a combination of the FEM and an integral equation using Green's function can be used to obtain both near and far fields at the antenna position. Of course, there must be free space between the integration plane and the antenna. Ground reflection can be treated by image theory. The electric field at the antenna position can be obtained from the following expression (Stratton [3])

$$\vec{E}(x',y',z') = \frac{1}{4\pi}\int_S [\, j\omega\mu(\vec{n}\times\vec{H})G + (\vec{n}\times\vec{E})\times\nabla G + (\vec{n}\cdot\vec{E})\nabla G\,]\cdot d\vec{s} \tag{13}$$

$\vec{E}(x',y',z')$ at an arbitrary position $P(x',y',z')$ outside the integration planes can be computed from (13). $\vec{H}$ and $\vec{E}$ on the right hand side of (13) are calculated by the FEM before the integration; G is the Green's function.

5 Validation of FEM code

5.1 Model for reflection and absorption computation

In order to confirm the accuracy of the FEM analysis using MAGNA/EMI, the reflection and absorption rates for a 28-GHz microwave, injected perpendicular to a lossy dielectric material (concrete), have been computed (Tanabe [4]). The reason for using the above frequency is that the analysis is applied to a system in which a concrete wall is subjected to a 28 GHz microwave generated by a gyrotron. Fig.1 shows the model for the analysis. The value of the electric field is normalized. The Coulomb gauge (9) was imposed on the magnetic vector potential. The conductivity and permittivity of the concrete are 0.19 [S/m] and $5\varepsilon_0$ [F/m], respectively. Absorbing layers are placed at the bottom of the concrete slab to model the 'infinite thickness' of the concrete. The value of σ was set to 15 [S/m] for the PML. The amplitudes of the electric and magnetic fields, the magnetic flux density and the Poynting vector in free space are 1 [V/m], 2.65×10^{-3} [A/m], 3.33×10^{-9} [T] and 1.34 [W/m^2], respectively, in the absence of concrete.

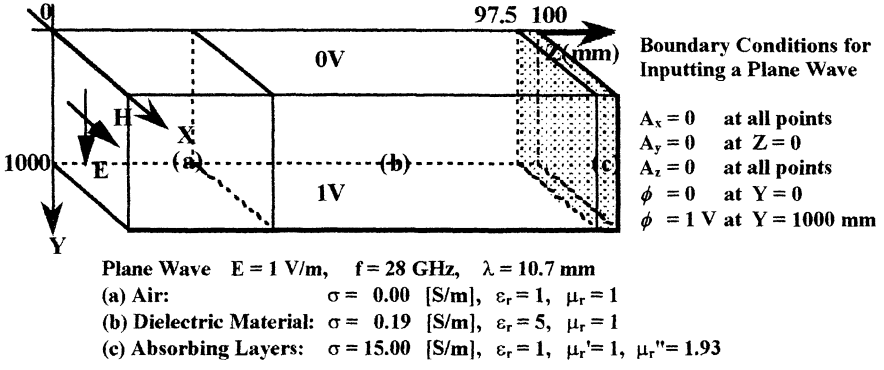

Figure 1 - Analysis model for concrete wall.

5.2 Comparison with analytic results

5.2.1 Reflection and absorption by concrete

Fig.2 shows the electric field at a given time. The wavelength of the incident wave is 1.07 mm. In the concrete, the wavelength is close to its value in free space while the wave impedance is given by

$$Z = \sqrt{\frac{\mu' - j\mu''}{\varepsilon' - j\varepsilon''}} = \sqrt{\frac{(\varepsilon'\mu' + \varepsilon''\mu'') + j(\varepsilon''\mu' - \varepsilon'\mu'')}{\varepsilon'^2 + \varepsilon''^2}}. \tag{14}$$

Since the imaginary parts of the concrete permittivity and permeability are $0.12\varepsilon_0$ and 0, respectively, the value of Z in the concrete is determined only by the real part of the permittivity. Z is almost 1/5 of the wave impedance in free space. In Fig.2, the ratio of the electric and magnetic fields in the concrete is 1/5 of its value in free space. Fig.3 shows the rms Poynting power density calculated from

$$|S_{rms}| = \frac{1}{2} Re(\vec{E} \cdot \vec{H}^*). \tag{15}$$

The skin depth for low conductivity materials is obtained analytically from

$$\xi = \frac{2}{\sigma}\sqrt{\frac{\varepsilon}{\mu}} \tag{16}$$

The Poynting power density decreases inside the concrete according to

$$e^{-\frac{2z}{\xi}} = e^{-z\sigma\sqrt{\frac{\mu}{\varepsilon}}} \approx e^{-32z} \tag{17}$$

At 72 mm it is 10% of its surface value, which agrees with the computed value.

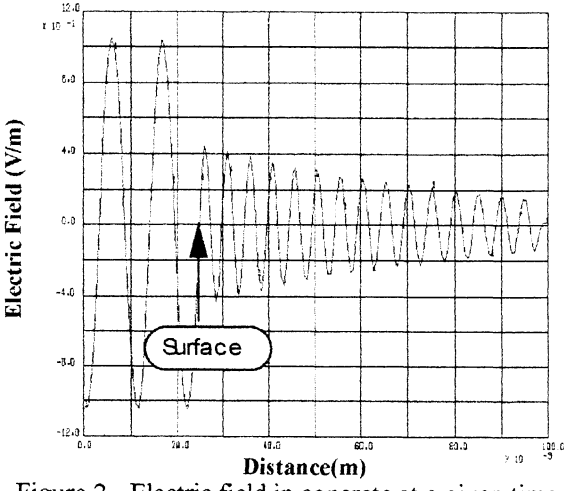

Figure 2 - Electric field in concrete at a given time.

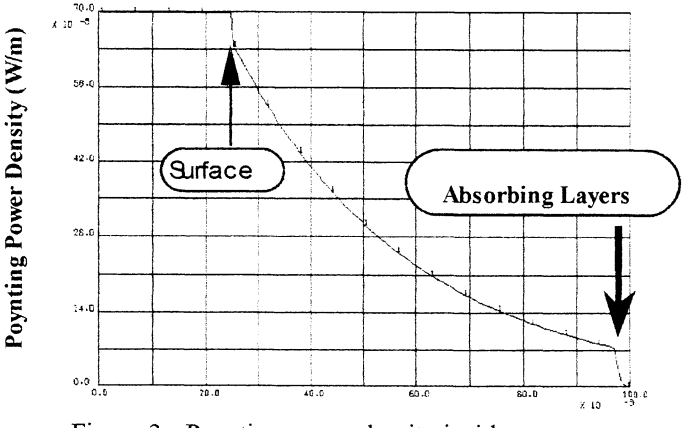

Figure 3 - Poynting power density inside concrete.

Fig.4 shows the time average electric field. The wavelength of the standing wave is half the wavelength of the propagating wave. The electric field node and the magnetic field loop of the standing wave appear at the surface of the concrete. From (16), the skin depth is 73 mm; from FEM it is 63 mm. Also from Fig.4, the VSWR is $S = 2.1$ so, the reflection coefficient obtained by FEM at the concrete surface is $\Gamma = 0.36$. This compares with $\Gamma = 0.38$ and $S = 2.22$ obtained from

$$\Gamma = \frac{\sqrt{\varepsilon/\mu} - \sqrt{\varepsilon_O / \nu_O}}{\sqrt{\varepsilon/\mu} + \sqrt{\varepsilon_O / \nu_O}} \tag{18}$$

$$S = \frac{1 + |\Gamma|}{1 - |\Gamma|} \tag{19}$$

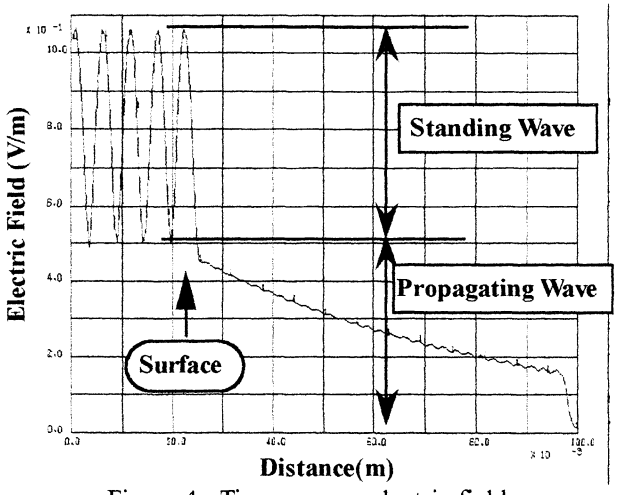

Figure 4 - Time average electric field.

5.2.3 Electromagnetic waves in metal

The skin depth is obtained analytically from the following equation

$$\xi = \sqrt{\frac{2}{\omega\sigma\mu}} \tag{20}$$

Fig.5 shows the attenuation of electric field in a 12-μm copper sheet (σ = 5.8×10^7 S/m) at 940 MHz (ξ = 2.1 μm). The solid line is analytical solution; the circles and triangles are FEM results with 40 and 4 layers, respectively. Even FEM results obtained with a coarse mesh (just 4 layers) are fairly accurate.

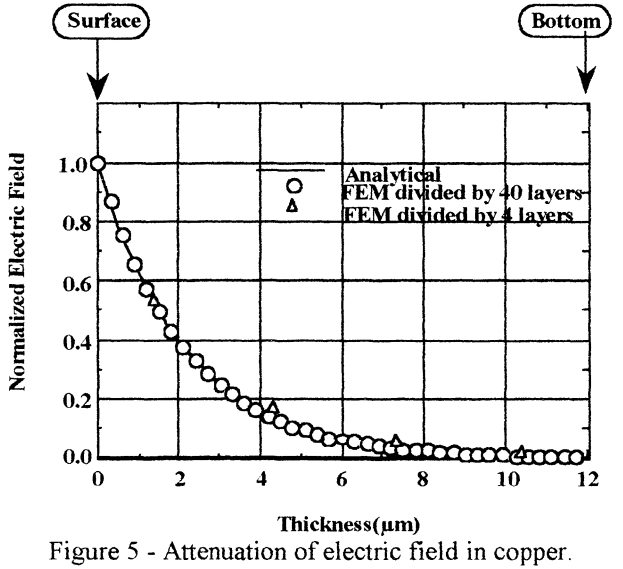

Figure 5 - Attenuation of electric field in copper.

6 Practical examples

MAGNA/EMI has been used for the design of PCB's and EM shields of various electronic products to prevent EMC problems. Two examples are shown in Figs. 6 and 7; one is related to cellular phone shield design, the other to the grounding of electronics inside a car.

In the cellular phone example, the emitted EM wave interferes with the phone's own PLL circuit for fixing the channel frequency. MAGNA/EMI was used to design a shield with reduced size and weight. The program can also compute the radiation pattern of the cellular phone and the induced currents and voltages on an electric circuit. Fig.6 shows the electric field distribution just above the PCB and the induced current density distribution.

In the second example, the interior of the car acts as a 'resonant cavity' for the noise EM fields. Using MAGNA/EMI, optimum grounding and harnessing has been designed. Fig.7 shows the electric field and current density distribution inside a generic car body.

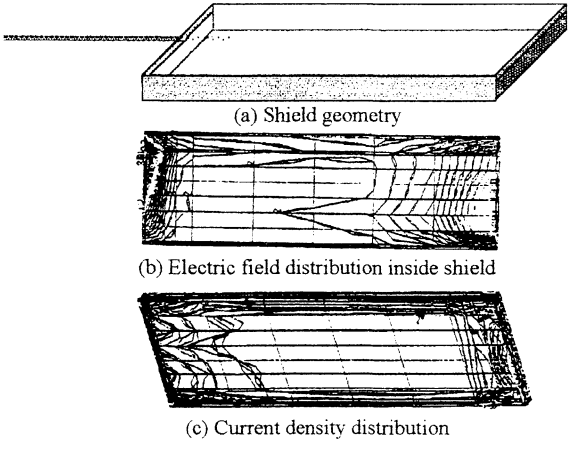

Figure 6 – Cellular phone shield problem.

7 Experience with equation solvers

For most practical EMI/EMC problems, bad aspect ratio finite elements are unavoidable because conducting shields and PCB's have relatively large surface areas and very small thickness. Therefore, a FEM program for EMI/EMC must be able to handle finite elements of rather poor geometrical aspect ratios (e.g. 1:100). In the examples given above, finite elements with aspect ratios far worse than 1:100 have been encountered. Nevertheless, acceptable accuracy has been maintained; this is evident from the accurate skin depth computation in spite of the presence of extremely poor aspect ratio finite elements in the model.

MAGNA/EMI features both Gauss elimination and ICCG equation solvers. For geometric aspect ratios exceeding 1:100, Gauss elimination is recommended.

There are also problems with poor electrical aspect ratios arising from large differences in material properties. Finite element models, which include high conductivity materials, often exhibit convergence difficulties with the ICCG solver, whereas Gauss elimination requires a lot of computer memory and CPU time. Nevertheless, even the most complicated, practical, three-dimensional EMI/EMC problems can be solved today by making use of Gauss-type equation solvers which exploit the advantages of today's high-speed virtual memory systems and ultra fast CPU's.

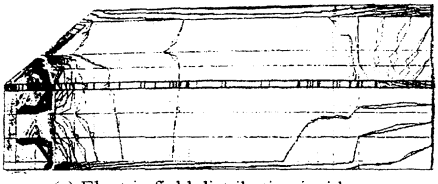

(a) Electric field distribution inside car

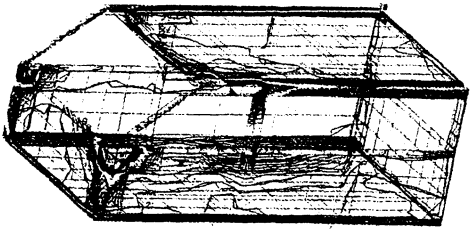

(b) Current density distribution on car body

Figure 7 – EM noise problem in car interior.

8 Conclusions

The accuracy of the FEM, with regard to the analysis of microwaves in low conductivity materials, is confirmed in this paper. Therefore, the method is useful for computing microwave reflection and absorption by complicated structures consisting of lossy dielectric materials such as concrete or even human tissue. It is also effective for EMI analysis of PCB's and conducting shields.

References

[1] Tanabe, S., et al., "Near and far fields analysis from flat cables," *Proc. IEEE 1997 EMCS*, pp.419-424, 1997.

[2] Berenger, J.P., "A perfect matched layer for the absorption of electro-magnetic waves," *J. of Computational Physics*, Vol.114, pp.185-200, (1994).

[3] Stratton, J.A., *Electromagnetic Theory*, McGraw-Hill, pp.464-467, 1941.

[4] Tanabe, S., and Murata, Y., "3D-FEM analysis for microwave reflection and absorption on/in dielectric materials with conductivity," *Proc. IEEE 1998 EMCS*, pp.602-607, 1998.